Type of contribution:
Editorial
▶ Research Paper
Case Study
Review Paper
Scientific Data
Report of Tech. Application

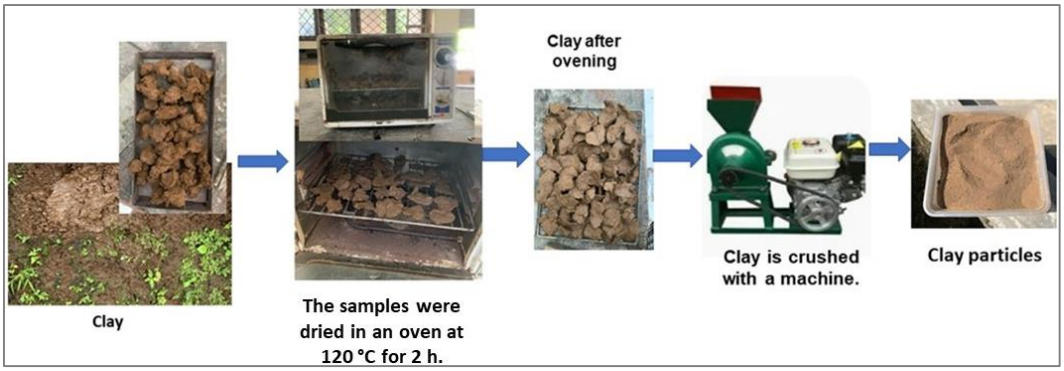
mesi
e-issn. 2798-5245

Mechanical Engineering for Society and Industry
Vol. 5, No. 2 (2025) pp 480-494
https://doi.org/10.31603/mesi.14144

Effect of calcination temperature on the thermo-structural behavior and morphology of natural clay for eco-friendly composite applications

Edi Syafri[1,2*a], Salman[3], Jamaluddin[1], Nasmi Herlina Sari[3*b], Suteja[3]

[1] Department of Agricultural and Computer Engineering, Politeknik Pertanian Negeri Payakumbuh, Payakumbuh 26271, **Indonesia**
[2] Research Collaboration Center for Nanocellulose, BRIN and Andalas University, Padang 25163, **Indonesia**
[3] Department of Mechanical Engineering University of Mataram, Mataram 83125, **Indonesia**
✉ edi.syafri@politanipyk.ac.id[a], n.herlinasari@unram.ac.id[b]



Highlights:

- CNCs were successfully produced from Pennisetum purpureum fibers using the ammonium persulfate (APS) oxidation method, an energy-efficient and eco-friendly process.
- APS oxidation effectively functionalized the CNCs surface, enhancing their solubility and dispersibility, crucial for their integration into nanocomposite materials.
- The study demonstrates the potential of agricultural waste, such as Pennisetum purpureum, as a renewable resource for sustainable material production.
- These findings pave the way for developing green materials with superior performance while reducing environmental impact.

Article info
Submitted: 2025-07-12
Revised: 2025-12-20
Accepted: 2025-12-28

This work is licensed under a Creative Commons Attribution-NonCommercial 4.0 International License

Publisher
Universitas Muhammadiyah Magelang

Abstract

Natural clay is a low-cost and abundant material with potential as a sustainable filler in composite applications. Although natural clay has been widely explored as a sustainable filler material, systematic studies correlating calcination temperature with simultaneous thermal, structural, and morphological evolution remain limited. This study aims to evaluate how different calcination temperatures affect the thermal, structural, morphological, and physical properties of natural clay to determine its suitability for eco-friendly composite use. Clay powders were thermally treated at 600 °C (CCB), 700 °C (CCG), and 800 °C (CCM), and comprehensively characterized using X-ray diffraction (XRD), Fourier-transform infrared spectroscopy (FTIR), thermogravimetric analysis (TGA), scanning electron microscopy (SEM), and physical testing. The results indicate that increasing calcination temperature significantly enhances crystallinity, and thermal stability, with the CCM sample (800 °C) exhibiting the most pronounced improvements. The CCM sample, calcined at 800 °C, exhibited the highest crystallinity index (72%), the lowest water absorption, the most compact microstructure, and the highest bulk density (6100 ± 40 kg/m³). TGA revealed improved thermal resistance up to 600 °C, with increasing char residue values from 38.2% (raw) to 48.2% (CCM), indicating enhanced thermal stability. FTIR analysis confirmed the reduction of hydroxyl and carbonate groups, particularly in the CCM sample. SEM observations showed a transformation from porous, irregular morphologies in raw clay to dense and homogeneous particles after calcination. These findings confirm that high-temperature calcined clay, especially

the CCM sample, presents excellent potential as a sustainable filler material for high-performance green composites.

Keywords: Calcined clay; Thermal treatment; Morphology; Crystallinity; Sustainable filler

1. Introduction

The development of green composite materials has been a key emphasis in materials science, as the demand for ecologically acceptable, low-cost, and outstanding performance alternatives to conventional fillers grows. Natural clays, particularly those rich in kaolinite, have sparked interest among mineral fillers due to their widespread availability, inexpensive cost, and thermally adjustable qualities [1], [2], [3], [4], [5].

Clay is a naturally occurring layered silicate mineral formed through the chemical weathering of silicate rocks, such as feldspar, under tropical and humid climates. Its primary composition consists of hydrated aluminosilicate particles (<2 µm), which exhibit plasticity when wet and harden upon drying or heating. These characteristics make clay a highly versatile material in a wide range of industrial applications, including ceramics, paper, paints, and polymer composite fillers. Kaolinite (a common clay mineral) comprises alternating tetrahedral silica and octahedral alumina sheets in a 1:1 configuration. This layered structure contributes to its high thermal stability and low cation exchange capacity, properties that make it especially suitable as a filler in polymer matrices. Recent studies demonstrate that incorporating kaolinite into polymer matrices (e.g., epoxy, polyester) composites enhances mechanical properties, such as tensile strength and stiffness, as well as thermal resistance and barrier performance against gases and moisture [6], [7]. Further modification through thermal activation (calcination) transforms kaolinite into amorphous metakaolin, a compound widely recognized for its reactivity and beneficial effects in composite systems. For instance, metakaolin-enhanced polymers have demonstrated superior mechanical performance and reduced structural degradation under thermal stress [8]. Similar findings were reported in geopolymers and alkali-activated binders using metakaolin, where samples calcined at 700–800 °C exhibited increased compressive strength, reduced CO_2 emissions, and improved thermal properties. Kaolinitic clays calcined at 650–800 °C undergo irreversible dehydroxylation that creates highly reactive, amorphous aluminosilicates with expanded specific surface area, an optimal chemical and structural state for use as fillers [9], [10].

Calcination, a typical procedure for modifying clay minerals, induces structural modifications such as dehydroxylation and phase shifts, which drastically alter the clay's physicochemical properties. In addition to being inexpensive and abundant in Indonesia, the clay calcination procedure has been shown to promote reactivity and surface roughness, boosting filler-matrix interactions [6], [11], [12]. When applied to polymer matrices, this change boosts clay particles' reactivity and compatibility. Recent research has demonstrated that calcined clay can increase the mechanical, thermal, and durability qualities of composite materials, making it an excellent choice for sustainable building and lightweight structural materials [8], [13]. Beyond polymer systems, calcined clay also plays a pivotal role in cementitious technologies. Koutsouradi *et al*. [14] compared laboratory-scale soak and flash calcination methods for LC^3 production and found that, when dehydroxylation degree and particle size are matched, both methods yield calcined clays with comparable physicochemical characteristics and compressive strength. In addition, Kalendova *et al*. [15] studied the use of clay minerals in polymer nanocomposites and silicate ceramics, highlighting that nanoscale delamination of kaolinitic platelets significantly improves tensile modulus, thermal stability, and barrier properties, while in ceramics, talc and kaolinite enhance strength and heat resistance. Recent studies by Khandelwal *et al*. [16] demonstrated that calcination of bentonite enhanced its surface area by 176%, which in turn improved interfacial bonding and led to a 48% increase in tensile strength and 90% reduction in wear when incorporated into basalt fiber–epoxy composites. These findings highlight the effectiveness of thermally activated clays as functional fillers for boosting mechanical performance and durability in polymer-based systems. Veriancova *et al*. [17] demonstrated that chemical modification of kaolin with silane and organic agents significantly enhances filler dispersion and interfacial bonding in rubber composites, leading to improved curing behavior and mechanical performance, findings that underscore the value of thermally or chemically modified clays as functional fillers in polymeric systems. Furthermore, Boakye *et al*. [18] discovered that calcination temperature influences the mechanical characteristics of polyester composites reinforced with palm fruit fibers, with specimens treated at 80°C for an hour having the highest tensile and bending strengths. Previous studies have consistently demonstrated that calcination temperature plays a critical role

in determining the final characteristics of calcined clays. Variations in calcination temperature can induce substantial changes in particle morphology, crystallinity, and surface area, properties that directly influence the performance of the resulting composite materials [19]. A comprehensive understanding of these changes, achieved through thermal, structural, morphological, and physical characterization techniques, is essential for optimizing the functionality of clay as a reinforcing filler. However, despite numerous studies on the use of clay in composite systems, few investigations have systematically examined the effect of different calcination temperatures on the physicochemical properties of natural clay particles. To the best of our knowledge, no previous study has comprehensively assessed the physicochemical transformations of natural clay subjected to a controlled range of calcination temperatures using multi-technique characterization, to evaluate its suitability as an eco-friendly filler in polymer composites.

Beyond chemical composition and mineralogical structure, particle shape is critical in determining the functional behavior of clay materials. When clay is employed as a filler material, particle shape, surface roughness, pore structure, and aggregation state all have a significant impact on its reactivity, packing efficiency, and interfacial interactions. Thermal treatment-induced morphological development can modify not just physical attributes such as density and water uptake, but also the efficiency of clay in reinforcing composite systems. Despite its relevance, the systematic relationship between calcination temperature and morphological modification of natural clay has received little attention, particularly in light of its prospective use as an eco-friendly filler material. Understanding how calcination-induced morphological changes occur is critical for maximizing clay performance in a variety of technical applications.

Therefore, this study aims to fill that gap by evaluating the thermal stability, crystallographic structure, surface morphology, and physical properties of calcined natural clay at varying temperatures (600 °C, 700 °C, and 800 °C), aiming to understand how these transformations impact its performance as a functional filler. Utilizing locally available clay resources in combination with simple thermal modification techniques, such as calcination, offers a promising pathway to reduce carbon footprint, production costs, and reliance on imported synthetic fillers. The findings from this study are expected to contribute fundamental insights into the development of lightweight and sustainable polymer composites using thermally modified natural clays as environmentally friendly fillers.

2. Material and Methods

2.1. Material

The natural clay used in this study was obtained from surface clay deposits located in Central Lombok, West Nusa Tenggara, Indonesia. The raw clay was collected in bulk and initially air-dried at ambient laboratory conditions for 72 h to reduce its moisture content. It was then oven-dried at 120 °C for 2 h to remove residual bound water. After drying, the clay was pulverized using a mechanical grinder and subsequently sieved through a 200-mesh screen (particle size < 75 µm) to ensure homogeneity in thermal treatment and consistency in subsequent characterization. The detailed steps of the initial preparation are illustrated in **Figure 1**.

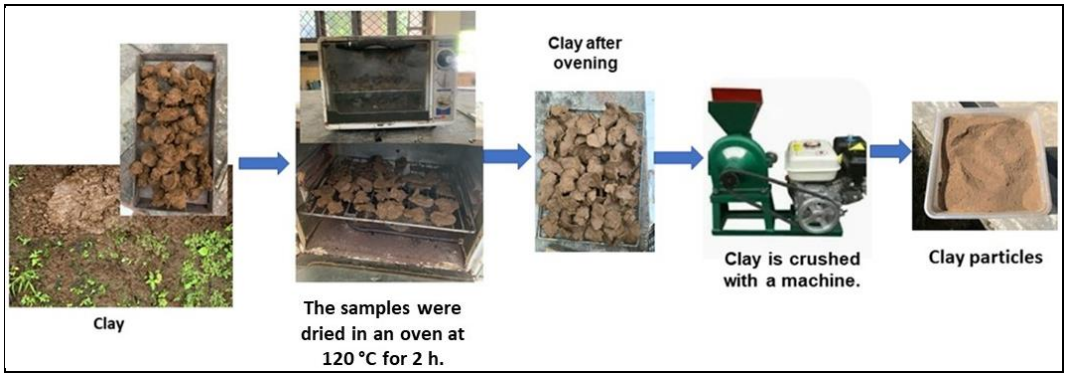


Figure 1. The process of preparing clay particles

2.2. Calcination Process of Clay

This study was conducted using an experimental approach to examine the effect of calcination temperature on natural clay properties. Data interpretation was based on comparative trend analysis, and formal one-way statistical testing was not performed.

In this process, the sieved clay powder was placed in a muffle furnace and calcined at three target temperatures: 600 °C, 700 °C, and 800 °C, each maintained for 2 h, as summarized in **Table 1**. The calcination duration of 2 h was selected based on previous studies reporting that this holding time is sufficient to achieve complete dehydroxylation and phase transformation of natural clay minerals without excessive grain growth. This duration was chosen to ensure structural stabilization while minimizing energy consumption. These calcination temperatures were selected to facilitate the removal of organic matter, induce structural transformations such as dehydroxylation and decarbonation, and enhance the physicochemical reactivity of the clay matrix [17]. After calcination, the samples were gradually cooled at room temperature to avoid thermal shock. The resulting calcined clays were then re-ground and re-sieved through a 200-mesh screen to ensure uniform particle size distribution. These samples were labeled as CCB (600 °C), CCG (700 °C), and CCM (800 °C) for subsequent analyses. The uncalcined sample was referred to as CCraw. A schematic representation of the complete calcination workflow is presented in **Figure 2**.

Table 1. Sample labels of clay before and after calcination at different temperatures (2 h holding time)

Sample codes	Description
CCraw	Clay particles without calcination
CCB	Clay particles after calcination at 600 °C for 2 h
CCG	Clay particles after calcination at 700 °C for 2 h
CCM	Clay particles after calcination at 800 °C for 2 h

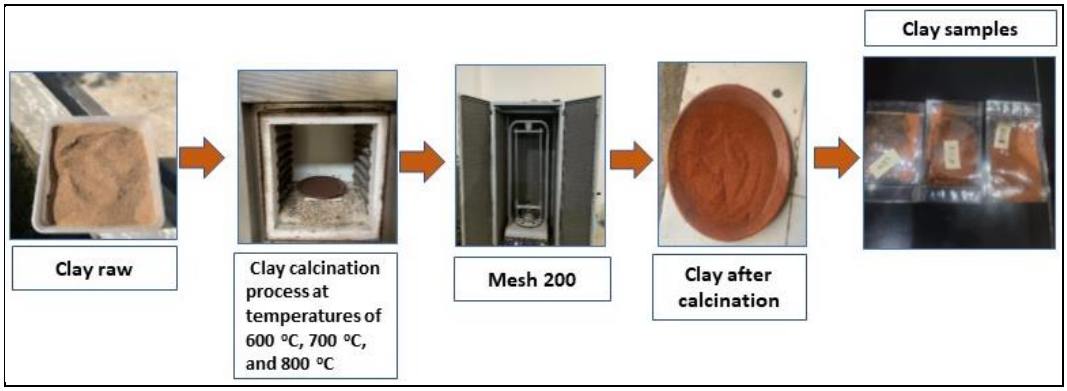


Figure 2. The calcination process of clay particles

2.3. Characterizations

2.3.1. Density

The density of calcined clay samples was determined according to the ASTM D578-79 standard using a pycnometer and toluene as the displacement medium. Prior to testing, the samples were dried in a desiccator with silica gel for 96 h to remove residual moisture and then ground into particles of approximately < 75 µm. To eliminate trapped air, the samples were immersed in toluene for 120 min in a borosilicate vessel. The density (ρ_{clay}) was calculated using Eq. (1) [20], [21].

$$\rho_{clay} = \left(\frac{(m_2 - m_1)}{(m_3 - m_1) - (m_4 - m_2)}\right) x\ \rho t \quad (1)$$

where: ρ sample = density of clay (kg/m³); ρ_t = density of toluene (866 kg/m³); m_1 = mass of empty pycnometer (kg); m_2 = mass of pycnometer with clay (kg); m_3 = mass of pycnometer with toluene (kg); m_4 = mass of pycnometer with clay and toluene (kg). Each reported value represents the mean of three independent measurements (n = 3), with standard deviation used to indicate data variability.

2.3.2. Chemical composition analysis

The chemical composition of the clay powders was analyzed using Scanning Electron Microscopy coupled with Energy Dispersive X-ray Spectroscopy (SEM–EDX). Prior to analysis, samples were oven-dried at 105 °C for 2 h to eliminate residual moisture that could interfere with imaging or electron interaction. A small amount of the dried powder was mounted onto a carbon adhesive tape fixed on an aluminum stub. If required, a thin conductive gold coating was applied using a sputter coater to enhance surface conductivity and image resolution during SEM examination. SEM observations were performed at an accelerating voltage of 15–20 kV under high-vacuum conditions. Elemental composition was analyzed on selected surface areas using the EDX detector integrated into the SEM system. The results were reported in terms of elemental weight percentage and atomic percentage, allowing comparison of major oxides and minor elements among the raw and calcined samples.

2.3.3. Water content test

The water content of the clay powder was measured using a standard oven-drying method. Approximately 5 g of each clay powder sample were weighed and placed in a laboratory drying oven at 105 ± 2 °C for 24 h to remove physically adsorbed moisture. After drying, the samples were transferred to a desiccator and cooled to room temperature to avoid moisture uptake from the ambient environment. The initial and final masses were recorded as W_{wet} and W_{dry}, respectively, using an analytical balance with 0.0001 g precision. The water content (*WC*) was calculated using the following Eq. (2) [21], [22], [23].

$$Water\ Content\ (WC)\ = \frac{W_{wet} - W_{dry}}{W_{dry}}\ x\ 100\% \quad (2)$$

2.3.4. Fourier Transform Infrared (FTIR) analysis

The functional groups present in the clay powders were analyzed using Fourier Transform Infrared (FTIR) spectroscopy with a PerkinElmer Frontier instrument. The samples, in powder form, were finely ground and mixed with potassium bromide (KBr) in an approximate ratio of 1:100 (sample: KBr by weight), then pressed into translucent pellets using a hydraulic press to form discs suitable for FTIR analysis. Spectra were recorded in the range of 4000–600 cm^{-1} with a spectral resolution of 4 cm^{-1}, and each spectrum was obtained by averaging 32 scans to improve accuracy and reduce noise. The resulting spectra were used to identify absorption bands associated with characteristic functional groups such as hydroxyl (–OH), silicate (Si–O), and carbonate (CO_3^{2-}). Changes in these functional groups were monitored to evaluate chemical transformations in the clay structure resulting from the calcination process at different temperatures.

2.3.5. Crystallinity index

The crystallinity index (*CI*) of samples was studied by X-Ray Diffraction (XRD) PANalytical. The XRD profile was recorded by diffractometer ray circuit. The radiation was CuKα at wave length 1.5406 Å. The ampere and voltage were operated at 30 mA and 40 kV, respectively. The 2θ degree was scanned in range 2–100° every 20°/min.

2.3.6. Morphology test by scanning electronic microscopy (SEM)-EDX

The surface morphologies of samples (CCB, CCG, and CCM) were observed by using a FEI model (Inspect–S50–type) scanning electron microscopy operating at 10 kV. Prior to testing, the samples were coated with gold sputtered for 5 min and equipped with a moving magnifier, which was used to capture images in order to examine the structural qualities of the composite material as whole. For each sample, SEM–EDX elemental analysis was conducted at three different regions on the particle surface (n = 3) to account for compositional heterogeneity. The reported elemental compositions represent the average values obtained from these measurements. Standard deviation values were calculated using the conventional statistical method based on the variability among the three independent EDX spectra.

2.3.7. Thermal Properties

A TG/DTA analyzer was used for thermogravimetric analysis (TGA). All samples were tested under nitro- gen atmosphere as heat source with 80 mL/min of speed. The test was done in range temperature 30–600 °C. The heating rate was 20 °C/min.

3. Results and Discussion

3.1. Chemical Composition Analysis

Each elemental composition value is presented as mean ± standard deviation, derived from three independent EDX measurements performed at different surface regions of the sample. The elemental analysis of clay powders before (CCraw) and after calcination at different temperatures (CCB: 600 °C, CCG: 700 °C, and CCM: 800 °C) revealed marked variations in the concentrations of major and minor elements. The primary components, oxygen (O), silicon (Si), and aluminum (Al), were consistent with typical aluminosilicate compositions. As presented in **Table 2**. Chemical composition of Clay Before and After Calcination at Different Temperatures (2 h holding time)**,** oxygen content increased from 42.97% in the raw sample to 50.58% in the CCM sample, indicating

enhanced formation of stable oxide phases as a result of kaolinite dehydroxylation and metakaolinite formation. This observation is in agreement with previous findings by Abubakar *et al*. [24] and Shah *et al*. [25], which highlighted the role of high-temperature treatment in promoting the release of structural water and the formation of amorphous, oxygen-rich phases. The aluminum content initially increased from 14.01% in CCraw to 18.57% in CCG, followed by a slight decrease to 14.02% in CCM. This trend reflects the intermediate activation of alumina phases and the possible redistribution or volatilization of Al species at higher temperatures, as also reported by Xue *et al*. [26]. Silicon levels remained relatively stable across all treatments (23.94–25.76%), with the highest value observed in CCM, suggesting preservation and slight rearrangement of the silicate network during calcination. This stability supports findings from Isabel Sánchez *et al*. [27], who emphasized the thermal robustness of silicate frameworks in clay minerals. Iron (Fe) concentration increased to 11.58% in CCG compared to 9.25% in CCraw, before decreasing to 8.17% in CCM, potentially due to partial oxidation followed by structural migration or phase transitions of iron oxides at elevated temperatures, in line with the mechanism described by Onyelowe *et al*. [28]. Minor elements such as calcium (Ca) and titanium (Ti) exhibited slight fluctuations. Ca increased from 0.55% to 0.65% and Ti from 1.01% to 1.39%, before both decreased again in the CCM sample. Though present in small quantities, these elements may influence surface activity and thermal behavior. Overall, the variations in chemical composition highlighted in **Table 2** reflect the significant effect of calcination on elemental distribution and surface chemistry, which enhances the potential of thermally treated clay as a functional filler for sustainable and energy-efficient composite materials.

Table 2. Chemical composition of clay before and after calcination at different temperatures (2 h holding time)

Samples	Mass (%)					
	O	Al	Si	Ca	Ti	Fe
CCraw	42.97 ± 1.0	14.01 ± 0.3	23.97 ± 0.6	0.55 ± 0.1	1.01 ± 0.2	9.25 ± 0.6
CCB	46.97 ± 1.1	17.01 ± 0.5	23.97 ± 0.6	0.59 ± 0.1	1.20 ± 0.2	10.25 ± 0.8
CCG	43.89 ± 1.3	18.57 ± 0.6	23.94 ± 0.7	0.63 ± 0.1	1.39 ± 0.2	11.58 ± 1.1
CCM	50.58 ± 1.1	14.02 ± 0.4	25.76 ± 0.6	0.65 ± 0.1	0.82 ± 0.7	8.17 ± 0.7

3.2. Density Analysis

Table 3 presents the bulk density values of clay samples before and after calcination at different temperatures, where a clear trend is observed. The raw clay (CCRaw) exhibited a density of 6090 ± 20 kg/m³, which increased slightly to 6120 ± 20 kg /m³ at 600 °C (CCB), and peaked at 6240 ± 10 kg/m³ at 700 °C (CCG). However, the density slightly decreased to 6100 ± 40 kg/m³ when the calcination temperature was further increased to 800 °C (CCM). The initial rise in density is primarily attributed to the progressive removal of hydroxyl groups and physically bound water from the clay structure, promoting the transformation of kaolinite into metakaolinite. This transformation leads to a more compact and ordered arrangement of particles, thereby reducing internal porosity and increasing mass per unit volume. The maximum density observed at 700 °C suggests an optimal balance between structural rearrangement and sintering, where the material achieves its highest level of compaction without initiating thermal degradation or excessive phase transformation.

At 800 °C, the slight decline in density is likely due to the development of closed micro-voids or the onset of recrystallization, which may introduce localized expansion in the microstructure. These thermal effects have been similarly reported by Shah *et al*. [25], who demonstrated that Limestone Calcined Clay Cement (LC³) systems containing calcined clay showed optimal densification and mechanical performance when calcination occurred around 700 °C. Irassar *et al*. [29] also observed that beyond this temperature range, the formation of secondary mineral phases could negatively affect the packing density of blended cements. From a materials engineering perspective, density is directly related to microstructural integrity, dimensional stability, and resistance to environmental degradation. High-density calcined clays reduce water absorption and permeability, which enhances durability, particularly in aggressive environments. Furthermore, using calcined clay as a partial clinker replacement in cementitious materials has demonstrated substantial environmental benefits, including a reduction of up to

Table 3. Density of clay before and after calcination at different temperatures (2 h holding time). Values are presented as mean ± standard deviation (n = 3)

Samples	Calcination temperatures (°C)	Density (kg/m³)	Water content (%)
CCraw	-	6090 ± 20	9.5 ± 0.3
CCB	600 °C	6120 ± 20	3.4 ± 0.2
CCG	700 °C	6240 ± 10	2.2 ± 0.2
CCM	800 °C	6100 ± 40	0.8 ± 0.3

40% in CO_2 emissions and lower embodied energy, as highlighted by Habert *et al*. [30] and Zunino *et al*. [31].

The observed changes in density with increasing calcination temperature are attributed to thermally induce mass loss and microstructural rearrangement rather than oxygen incorporation. During calcination, dehydroxylation and the removal of physically bound water reduce the overall mass of the material, while simultaneous particle rearrangement and pore collapse promote densification. As a result, the apparent density increases despite the absence of chemical oxygen uptake.

The CCG sample calcined at 700 °C, with its optimal density and structural properties, is especially suitable for use as a filler in green construction materials such as LC^3 cement, alkali-activated geopolymers, and 3D-printed building elements that require dimensional precision and long-term stability. Meanwhile, the CCM sample, despite a minor reduction in density, may still be considered for specialized ceramic applications or thermally insulating composites due to its controlled microporosity. These findings reinforce the importance of thermal optimization in tailoring the physical characteristics of calcined clays for specific functional applications.

The calcined clay's pore structure is inextricably linked to its density and water content. As calcination temperature rises, pore volume and connectivity decrease due to particle rearrangement and partial pore collapse, resulting in a denser material framework. This reduction in accessible porosity reduces the material's ability to retain water, resulting in lower water content values. As a result, the observed negative connection between density and water content indicates microstructural consolidation rather than compositional changes, underscoring the importance of calcination-induced morphological evolution.

3.3. Water Content Analysis

Table 3 clearly demonstrate a significant reduction in water content as the calcination temperature increases. The raw clay (CCraw) exhibited a water content of 9.5 ± 0.3%, which is typical for naturally occurring kaolinitic clays that retain both adsorbed and interlayer water due to their hydrophilic nature and fine particle size. Upon calcination at 600 °C (CCB), the water content dropped to 3.4 ± 0.2%, indicating partial removal of physically adsorbed moisture and the onset of dehydroxylation processes. Further heating to 700 °C (CCG) reduced the moisture to 2.2 ± 0.2%, suggesting continued breakdown of hydroxyl-bearing phases. At 800 °C (CCM), the lowest moisture content was observed (0.8 ± 0.3%), consistent with nearly complete dehydroxylation and the formation of amorphous metakaolinite. The observed thermal dehydration behavior can be attributed to the sequential elimination of water molecules from both the surface and internal structure of the clay. The initial mass loss, occurring below 150 °C, corresponds to the evaporation of physically adsorbed water. This is followed by a more significant weight reduction between 400 and 600 °C, which is associated with the dehydroxylation process, specifically the release of structurally bound hydroxyl groups within the kaolinite lattice. These transformations have been consistently documented in differential thermal analysis DTA/TGA studies, including the findings reported by Derouiche *et al*. [32]. The near-zero water content in the CCM sample confirms that most hydroxyl functionalities have been thermally eliminated, a key indicator of the formation of reactive amorphous phases.

These findings align well with the observations reported by Feriancová *et al*. [17], who found that kaolin treated at 800 °C exhibited a sharp decline in water retention, supporting its conversion to metakaolin. Similarly, Khandelwal *et al*. [16] observed that bentonite clays subjected to thermal treatment showed substantial reduction in moisture content, which corresponded with improved dimensional stability and thermal performance in composite matrices. The study by Koutsouradi *et al*. [14] also emphasizes that the calcination of clay for cement and composite applications significantly improves its moisture stability, which is critical for consistent processing and performance. From an application standpoint, the reduced water content in calcined clays is advantageous for polymer composite fabrication, as it minimizes moisture-induced degradation, void formation, and weak interfacial bonding during processing. In particular, the CCM sample, with its lowest residual moisture, is highly suitable as a thermally stable filler in moisture-sensitive systems such as thermoset resins, geopolymer matrices, or biodegradable composites, where dimensional stability and long-term durability are essential.

3.4. Fourier Transform Infra-Red (FTIR) Analysis

Infrared spectroscopy was performed to assess the modifications in molecular bonding and structural groups in raw and heat-treated clay powders. **Figure 3** show the FTIR of different samples.

The FTIR spectra of CCraw and calcined samples (CCB, CCG, and CCM) showed marked alterations across key vibrational regions. The high-wavenumber peaks around ~3775 cm^{-1} (raw), ~3785 cm^{-1} (CCG), and ~3755 cm^{-1} (CCM) correspond to inner hydroxyl groups of kaolinite. These peaks weaken progressively with higher calcination temperatures, consistent with dehydroxylation and transformation into metakaolinite, as also observed by recent studies heating clays between 600 and 800 °C. Water-related absorptions, including the broad O–H stretch between 3458–3435 cm^{-1} and the H–O–H bending band at ~1638 cm^{-1}, were significantly reduced following calcination, reflecting effective moisture and lattice water removal. New peaks between 2378–2344 cm^{-1} emerged in heated samples, likely due to CO_2 adsorption or carbonate intermediates formed during thermal decomposition, an effect noted in published kaolinite thermolysis research. That strengthened band around 1065 cm^{-1}, tied to Si–O–Si and Si–O–Al network vibrations, became sharper and more intense after heating, indicating greater ordering within the silicate framework. This aligns with findings from Anove *et al*. [33], who observed a more prominent silicate absorption near 1080 cm^{-1} upon calcination at 750 °C.

Peaks in the lower range (795–800 cm^{-1} and ~693 cm^{-1}), which are related to Si–O bending modes of quartz and residual kaolinite, diminished in intensity and slightly shifted position, pointing toward partial amorphization and structural alteration. Additional absorption peaks near 570–543 cm^{-1} and 458–464 cm^{-1}, attributed to Al–O and Si–O bending vibrations, became more pronounced following heat treatment, indicating microstructural restructuring of the aluminosilicate network. These spectral changes support the hypothesis that calcination mobilizes hydroxyl groups while preserving crucial silicate linkages—key for improving the chemical compatibility of clay within composite matrices [34].

Notably, at 800 °C (CCM), all silanol and aluminol peaks had diminished, confirming full dehydroxylation and transition into an amorphous metakaolinitic phase. However, Si–O absorptions persisted, indicating that the silicate skeleton remains intact, findings consistent with those reported by Zunino and Scrivener [35] and Anove *et al*. [33], who also observed persistent Si–O features post-calcination. In conclusion, the FTIR results definitively show elimination of hydroxyl and water-related groups and increased clarity in silicate spectral bands, supporting structural rearrangement and dehydration processes in the clays. These changes are essential in enhancing the structural integrity and reactivity of calcined clays for use in sustainable composite applications. The specific band assignments are detailed in **Table 4**.

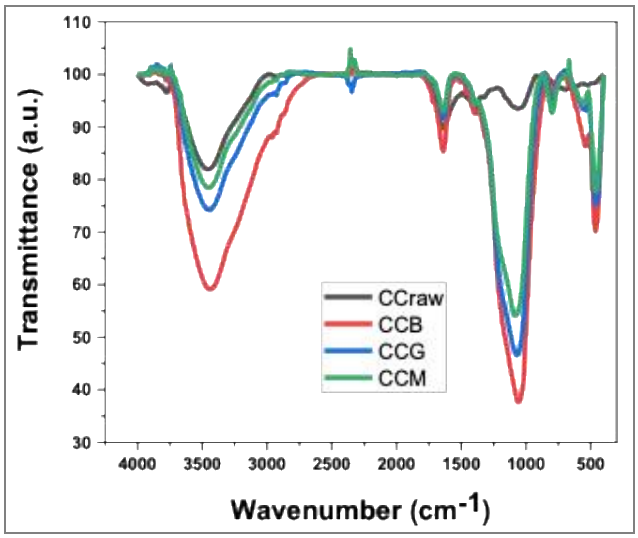


Figure 3. FTIR of clay before and after calcination at different temperatures

Table 4. Clay's FTIR spectrum properties both before and after calcination

Wave number (cm^{-1})				Assignments
CC-Raw	CCB	CCG	CCM	
3775	3756	3785	3755	Stretching vibration of inner-surface –OH groups (kaolinite)
3458	3445	3435	3449	Stretching vibration of adsorbed water (O–H)
-	2378	2346	2344	Asymmetric stretching of CO_2 (carbonate presence or surface-adsorbed CO_2)
1637	1639	1071	1082	Bending vibration of molecular water (H–O–H)
1398	1509	795	800	Vibrations of carbonate or residual organics
1064	1059	543	570	Si–O–Si or Si–O–Al asymmetric stretching vibrations (silicate structure)
693	795	458	464	Out-of-plane bending of Si–O (quartz/kaolinite)
-	540.1	543	570	Deformation vibrations of Al–O and Si–O bonds

3.5. Crystallinity Index

Figure 4 presents the X-ray diffraction (XRD) patterns of raw clay (CCraw) and calcined clay samples treated at 600 °C (CCB), 700 °C (CCG), and 800 °C (CCM). The diffraction pattern of CCraw exhibits broad and relatively low-intensity peaks, particularly around 2θ = 12.3°, 20.1°, and 26.6°, which are characteristic of kaolinite and quartz minerals. The broadness of these peaks suggests a significant amorphous phase and low crystalline order, typical of unprocessed natural clays.

Upon calcination at 600 °C (CCB), the peak intensity increases, especially in the region near 2θ = 20–30°, indicating partial structural reorganization and the beginning of dehydroxylation of kaolinite. This structural collapse transforms kaolinite into metakaolinite, an amorphous aluminosilicate phase. The diffraction peaks become sharper and more defined in the CCG (700 °C) and CCM (800 °C) samples, reflecting increased structural rearrangement and short-range ordering within the matrix.

The Crystallinity Index (CrI) calculated using the Segal method, based on the ratio of the maximum (002) peak (I_{oo2}) and the amorphous baseline intensity (I_{am}), confirms this trend. CrI increases from approximately 37.5% in CCraw**,** to 57.1% in CCB**,** 66.7% in CCG**,** and 72.0% in CCM, as display in Table 5. These results indicate that calcination promotes the formation of a more ordered structure without forming fully crystalline new phases such as mullite, which typically emerges above 900 °C.

The thermal-induced transformations are in agreement with previous findings by Zunino *et al*. [31], who noted that calcination at 700–800 °C optimally enhances structural ordering and stability in metakaolinite without compromising its reactivity. In addition**,** Zunino and Scrivener [35] reported that XRD patterns of calcined kaolinitic clays at similar temperatures exhibited increased crystallinity while preserving the amorphous features essential for pozzolanic or composite applications.

The high CrI observed in CCM (800 °C) reflects a suitable balance between amorphous content and ordered domains, which is advantageous for composite reinforcement. The enhanced microstructural integrity contributes to improved thermal stability, reduced water uptake (as seen in density and moisture absorption data), and better interfacial bonding when used in polymer or cementitious matrices. Overall, the XRD analysis confirms that thermal activation via calcination significantly modifies the structural framework of clay particles, with the most optimal balance of crystallinity and reactivity achieved at 800 °C. This reinforces the potential of thermally treated clay as a sustainable and functional filler for advanced composite materials.

While the CCM sample calcined at 800 °C exhibits the highest crystallinity and most compact morphology, such characteristics may not be universally advantageous for all applications. In highly reactive systems such as geopolymerization, excessive structural ordering and reduced amorphous content can limit the availability of reactive aluminosilicate species, thereby decreasing dissolution kinetics and overall reactivity. This suggests that although high-temperature calcination enhances thermal and structural stability, it may compromise chemical reactivity in alkali-activated systems. Therefore, the optimal calcination temperature should be selected based on the intended application. Moderate calcination temperatures may provide a balanced combination of reactivity and structural integrity, whereas higher temperatures are more suitable for applications requiring enhanced thermal stability and dimensional robustness, such as polymer composites and ceramic fillers.

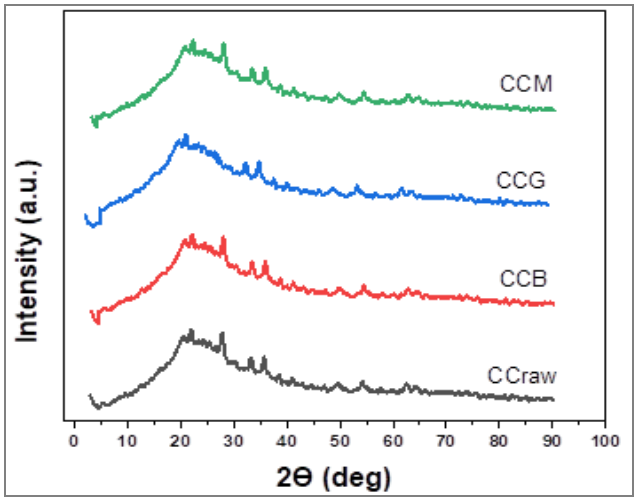


Figure 4. The Crystallinity Index of clay before and after calcination at different temperatures

Sample Codes	CrI (%)
CCraw	37.5%
CCB (600°C)	57.1%
CCG (700°C)	66.7%
CCM (800°C)	72.0%

Table 5. The crystallinity index of clay raw, CCB, CCG and CCM samples

3.6. Morphology Analysis

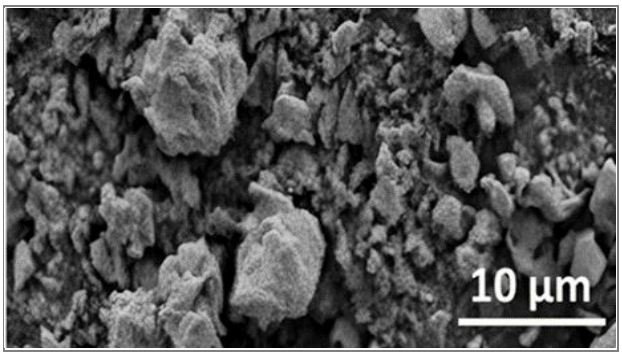


Figure 5. SEM image of clay raw [36]

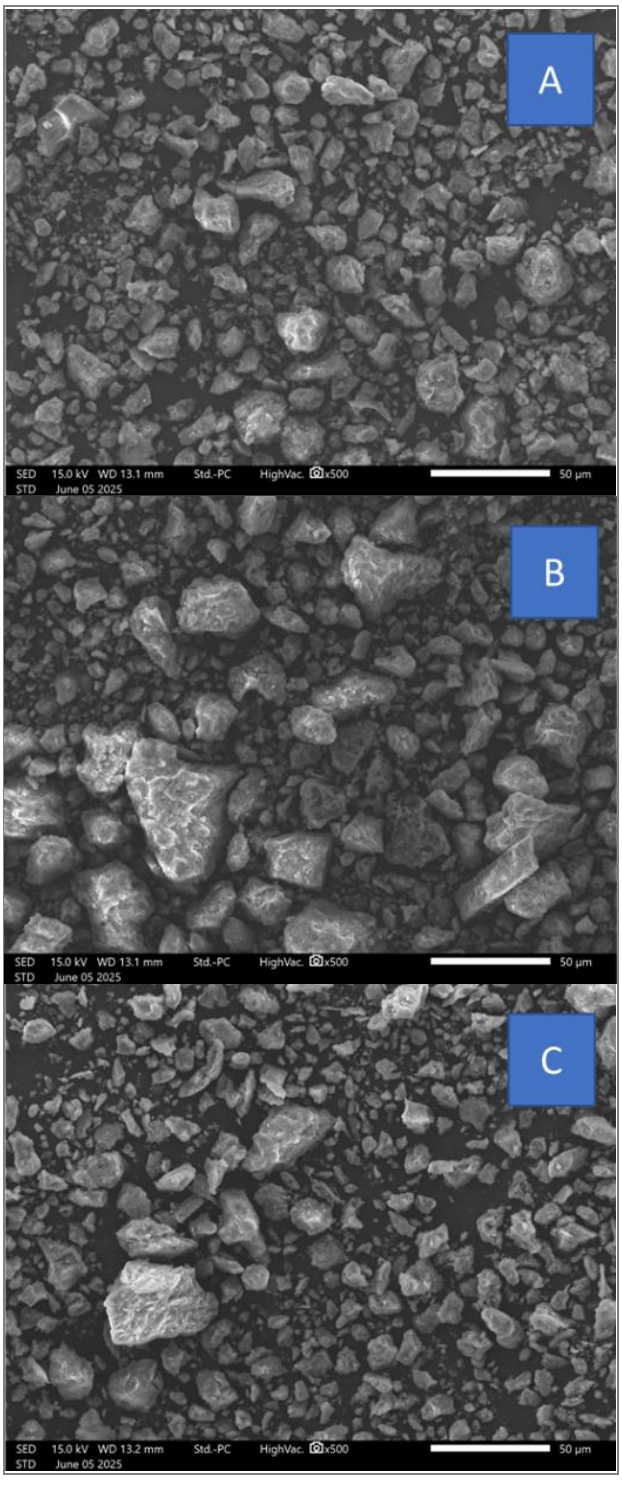


Figure 6. SEM images of clay calcination samples: (a) CCB; (b) CCG; and (c) CCM

The morphology of calcined clay samples was analyzed using SEM to evaluate the structural changes induced by thermal treatment. Direct SEM observation of the raw clay (CCraw) was not conducted in this study. Therefore, the morphological characteristics of CCraw were discussed based on the recent work of Gu and Ling *et al*. [36], who reported that untreated natural clay typically exhibits irregular particle shapes, loosely packed structures, and pronounced interparticle voids (**Figure 5**). This morphology is indicative of moderate crystallinity and high moisture affinity, characteristics that justify selecting this clay for calcination [36].

SEM micrographs of calcined samples (**Figure 6a**–**Figure 6c**) highlight notable morphological evolution. The CCB sample (600 °C) (**Figure 6a**) shows partial separation of layered particles, suggesting early dehydroxylation. In the CCG (**Figure 6b**), clear particle boundaries and enhanced fragmentation appear, reflecting the formation of amorphous metakaolinite with increased specific surface area, traits beneficial for composite bonding. The CCM sample (**Figure 6c**) displays finely distributed, angular particles with a more homogeneous morphology, indicating complete dehydroxylation and phase transformation due to intensive thermal treatment.

These morphological developments are consistent with reports by Nasiri *et al*. [37], who observed increased surface roughness and reactivity in calcined kaolinitic clays. Yi-Sheng Wang *et al*. [38] and Hanein *et al*. [12] further confirmed that calcination enhances specific surface area and wettability, improving filler–matrix interfacial bonding in polymer-based composites.

The microstructural evolution observed after calcination is expected to play a significant role in the long-term durability of composite materials. The reduction in porosity and increased particle densification, particularly in the CCM sample, may limit moisture ingress and reduce

interfacial degradation when incorporated into composite systems. Lower pore connectivity can hinder water diffusion pathways, which is a critical factor governing hydrolytic degradation and dimensional instability under humid environments.

Although this work did not include polymer-based composite testing, the observed morphological and surface properties of the calcined clay suggest the possibility of better filler-matrix interaction. When employed as filler materials, calcination increases surface roughness, reduces agglomeration, and modifies surface chemistry, all of which improve mechanical interlocking and interfacial contact. These inferences are based on proven structure-property connections described in the literature and should be considered indicative rather than conclusive. Validating these predictions requires direct examination through polymer-clay composite production and interfacial testing.

3.7. Thermal Stability Analysis

Figure 7a presents the thermogravimetric analysis (TGA) curves of raw clay (CCraw) and calcined clay samples at 600 °C (CCB), 700 °C (CCG), and 800 °C (CCM), highlighting their thermal decomposition behavior. All samples exhibited a multi-stage weight loss profile. The initial mass loss observed between 30–150 °C is attributed to the evaporation of physically adsorbed water. This loss was most prominent in the CCraw sample, indicating its highly hydrophilic surface and higher moisture retention. In contrast, the calcined samples, particularly CCM, demonstrated significantly reduced moisture loss in this range, reflecting the effective removal of surface hydroxyl and adsorbed water groups during calcination. The second stage of mass reduction, occurring between 200–400 °C, corresponds to the decomposition of organic matter and the onset of dehydroxylation in clay minerals such as kaolinite. The diminishing intensity of this event in calcined samples indicates that most of the volatile components were already eliminated during the calcination process. This observation aligns with Derouiche *et al*. [32], who reported similar thermal degradation behavior in phosphate-based geopolymers utilizing calcined clay at 800 °C. The third phase, from 400 to 600 °C, involves further dehydroxylation and partial decomposition of residual carbonates. In calcined samples, this stage was marked by a more gradual slope in the TGA curves, demonstrating increased thermal stability. Notably, the final residue content increased progressively from CCraw (35.17%) to CCB (38.22%), CCG (40.32%), and reached its peak in CCM (48.2%), suggesting that higher calcination temperatures enhance the formation of thermally stable structures.

This increase in thermal stability can be attributed to the irreversible transformation of kaolinite into amorphous metakaolinite and spinel-type phases, accompanied by the elimination of structural –OH groups and volatile compounds. As explained by Salahudeen [39], these transformations occur predominantly between 600–900 °C and result in a more robust aluminosilicate network. Among the tested samples, CCM exhibited the highest thermal stability, confirming its suitability as a thermally stable filler for sustainable composite materials. The enhanced thermal resistance not only improves the performance of composites during high-temperature processing but also contributes to dimensional stability, mechanical durability, and overall longevity of the final product. This makes calcined clay, especially at 800 °C, an attractive candidate for green filler applications in thermally demanding environments.

Figure 7b illustrates DTA curves for the raw clay (CCraw) and the calcined variants (CCB, CCG, CCM), showcasing thermal events that correlate with structural and compositional transformations. An initial broad endothermic dip below 100 °C is observed, associated with the release of physically adsorbed water. The magnitude of this peak diminishes after calcination—particularly in CCG and CCM—indicating successful removal of moisture, consistent with findings by Kosmidi *et al*. [40], who reported similar water loss behavior in thermally activated kaolinitic clays. Between approximately 450–600 °C, an intense endothermic peak mark the dehydroxylation process where structural hydroxyl groups are removed, converting kaolinite into metakaolinite. In CCraw, this transition appears around 550–580 °C; in calcined samples, the shift toward lower temperatures and sharper peak profiles indicates enhanced structural order due to prior thermal activation. This thermogram behavior aligns with observations by Xue *et al*. [26], who documented improved peak definition and earlier aluminosilicate dehydroxylation following pre-calcination.

Notably, no exothermic peaks were observed in the 800–1000 °C range, suggesting that full recrystallization into mullite or spinel phases had not yet occurred, confirming that 800 °C is below the threshold for such transformations. This observation is in agreement with thermogram studies on kaolinitic clays from San José (Oruro), where the onset of spinel-like or mullite phase formation begins above ~880 °C [41]. These thermal events support a mechanistic model where calcination

removes moisture and hydroxyl groups, creating a more reactive metakaolinite structure while retaining amorphous aluminosilicate phases. This structural rearrangement is crucial for pozzolanic activity and the long-term thermal stability of composites. The refined pattern observed in CCG and CCM, featuring distinct, narrower peaks, suggests that pre-calcination enhances ordering, improving sintering behavior and interfacial bonding in subsequent composite applications. Moreover, avoiding high-temperature recrystallization prevents porosity increase and preserves reactive phases, making calcined clays excellent supplementary cementitious materials (SCMs) for low-carbon construction systems such as LC³ [41].

In addition to the major aluminosilicate constituents, minor mineral impurities such as Fe, Ca, and Ti were detected by SEM–EDX analysis. These elements are commonly present in natural clays and may influence both thermal behavior and final application performance. Iron-containing phases can act as fluxing agents during calcination, potentially facilitating phase transformation and promoting densification at elevated temperatures. Similarly, calcium-bearing compounds may contribute to partial vitrification or affect the formation of secondary phases, influencing thermal stability and mechanical performance. Titanium, although present in small amounts, may enhance chemical resistance and contribute to microstructural refinement. While the concentrations of these impurities are relatively low, their presence should be considered when tailoring calcined clay for specific applications, as they may impart beneficial or adverse effects depending on the processing conditions and target matrix.

The calcination-induced morphological and elemental composition changes indicate that the treated clay is not limited to a particular application system. Reduced agglomeration, modified surface texture, and the presence of stable aluminosilicate phases may allow compatibility with a wide range of polymeric matrices, such as thermosetting and thermoplastic systems, and also inorganic matrices like cementitious and ceramic materials. These properties suggest that calcined clay has the ability to ser ve as a versatile filler or reinforcing phase, provided that the target matrix's processing conditions and interfacial methods are followed.

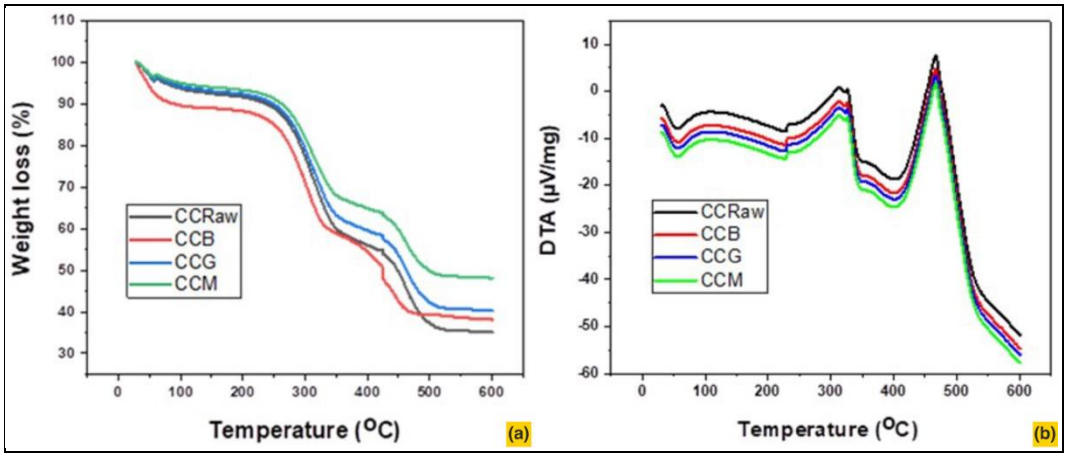


Figure 7. (a) TGA; (b) DTA of clay before and after calcination at different temperatures

4. Conclusion

This study demonstrates that increasing calcination temperature systematically alters the thermal stability, structural ordering, and morphological characteristics of natural clay. Calcination at different temperatures—600 °C for CCB, 700 °C for CCG, and 800 °C for CCM—significantly enhanced the structural, thermal, morphological, and physical properties of the clay powders, with CCM showing the most favorable results. The CCM sample exhibited the highest crystallinity index (72%), outperforming CCB and CCG, indicating more effective phase transformation at higher calcination temperature. FTIR spectra showed a more complete removal of hydroxyl and carbonate groups in CCM. TGA analysis revealed a clear trend of increased thermal stability with rising calcination temperature, as shown by char residue values of 38.22% (CCB), 40.32% (CCG), and 48.2% (CCM), all stable up to 600 °C. Furthermore, CCM displayed the highest bulk density (6100 ± 40 kg/m³) and the lowest water absorption, suggesting improved compaction and moisture resistance compared to CCB and CCG. SEM analysis confirmed that CCM had the most compact and homogeneous microstructure. These findings confirm that calcination at 800 °C (CCM) produced the most optimized clay, making it a strong candidate for use in sustainable composites, ceramics, and environmental materials, with further research needed to tailor

performance for specific applications. Despite these promising results, this study has several limitations. Long-term durability under environmental exposure, such as moisture ingress and thermal cycling, was not evaluated. In addition, direct fabrication and testing of clay-reinforced polymer composites were not conducted, limiting the ability to experimentally validate filler–matrix interfacial performance. Future research should focus on tailoring the calcination process to specific application needs, such as geopolymer synthesis, polymer-clay composites, or pollutant adsorption, while incorporating life cycle assessment (LCA) and techno-economic analysis to evaluate scalability and sustainability. This approach will support the development of environmentally responsible and high-performance clay-based materials for diverse industrial sectors.

Acknowledgements

The authors gratefully acknowledge the support provided by the Ministry of Higher Education, Science and Technology of the Republic of Indonesia (Kemdiktisaintek) through the Competitive Grant under the Fundamental Research Program for the fiscal year 2025 (PFR grant number: 2034/PL25/AL.04/2025).

Authors' Declaration

Authors' contributions and responsibilities - Edi Syafri: Supervision, Conceptualization, Methodology, Investigation, Writing – original draft, formal analysis; Salman, Jamaludin: Methodology, Conceptualization, Investigation, Data curation, Visualization; Nasmi Herlina Sari: Validation, Writing - Review & Editing; Suteja: Resources, Project administration.

Funding – Ministry of Higher Education, Science and Technology of the Republic of Indonesia (Kemdiktisaintek) through the Competitive Grant under the Fundamental Research Program for the fiscal year 2025 (PFR grant number: 2034/PL25/AL.04/2025).

Availability of data and materials - All data is available from the authors.

Competing interests - The authors declare no competing interests.

Additional information – No additional information from the authors.

References

[1] C. Sudswong, "Effects Of Calcined Clay On Properties Of Mortar And Concrete," Sirindhorn International Institute Of Technology Thammasat University, 2022.

[2] E. Syafri *et al.*, "Effect of ultrafine grinding and ultrasonication duration on the performance of polyvinyl alcohol (PVA) agave gigantea cellulose micro fiber (CMF) bio-composite film," *Journal of Natural Fibers*, vol. 20, no. 1, 2023, doi: 10.1080/15440478.2023.2192545.

[3] N. Herlina Sari *et al.*, "Exploring the impact of water soaking on the mechanical, thermal, and physical properties of Paederia foetida fiber stem biocomposites: A study in sustainable material innovation," *Case Studies in Chemical and Environmental Engineering*, vol. 10, Dec. 2024, doi: 10.1016/j.cscee.2024.100977.

[4] N. Herlina Sari *et al.*, "Fabrication of bio-fiber based Eichhornia crassipes/Al2O3 particles hybrid biocomposites and investigation of important properties," *Proceedings of the Institution of Mechanical Engineers, Part E: Journal of Process Mechanical Engineering*, 2023, doi: 10.1177/09544089231167750.

[5] E. Syafri *et al.*, "Characterization and properties of cellulose microfibers from water hyacinth filled sago starch biocomposites," *International Journal of Biological Macromolecules*, vol. 137, pp. 119–125, 2019, doi: 10.1016/j.ijbiomac.2019.06.174.

[6] N. Relosi and S. R. Kunst, "Effect of addition of clay minerals on the properties of epoxy / polyester powder coatings," *Polímeros,* vol. 28, no. 4, pp. 1–27, 2018.

[7] A. Gürses and K. Güne, "Preparation of Polyethylene Clay Composites via Melt Intercalation Using Hydrophobic and Superhydrophobic Organoclays and Comparison of Their Textural , Mechanical and," *Polymers*, vol. 16, no. 272, pp. 1–13, 2024.

[8] Y. Zhang and H. Le Ferrand, "Bioinspired Self-Shaping Clay Composites for Sustainable

Development," *biomimetics Article*, vol. 7, no. 13, pp. 1–15, 2022.

[9] M. F. Mubarak, M. A. Zayed, A. Nafady, and A. E. L. Shahawy, "Fabrication of Hybrid Materials Based on Waste Polyethylene/Porous Activated Metakaolinite Nanocomposite as an Efficient Membrane for Heavy Metal Desalination Processes," *Adsorption Science and Technology*, vol. 2021, 2021, doi: 10.1155/2021/6695398.

[10] T. M. Zewdie, I. Prihatiningtyas, A. Dutta, and N. G. Habtu, "Characterization and benefi ciation of Ethiopian kaolin for use in fabrication of ceramic membrane," *Materials Research Express*, vol. 8, no. 11, p. 115201, 2021, doi: 10.1088/2053-1591/ac2f75.

[11] T. Shi *et al.*, "Calcined Attapulgite Clay as Supplementary Cementing Material : Thermal Treatment , Hydration Activity and Mechanical Properties," *International Journal of Concrete Structures and Materials*, vol. 16, no. 10, pp. 1–10, 2022, doi: 10.1186/s40069-022-00499-8.

[12] T. Hanein *et al.*, "Clay calcination technology : state-of-the-art review by the RILEM TC 282-CCL," *Materials and Structures*, vol. 55, no. 3, pp. 1–15, 2023, doi: 10.1617/s11527-021-01807-6.

[13] N. Relosi, O. A. Neuwald, A. J. Zattera, D. Piazza, and S. R. Kunst, "Effect of addition of clay minerals on the properties of epoxy / polyester powder coatings," *Polimeros*, vol. 5169, no. 4, pp. 355–367, 2018.

[14] A. Koutsouradi *et al.*, "Impact of clay calcination method on the physicochemical properties of limestone calcined-clay cement," *Construction and Building Materials*, vol. 473, p. 140939, 2025, doi: 10.1016/j.conbuildmat.2025.140939.

[15] A. Kalendova, J. Kupkova, M. Urbaskova, and D. Merinska, "Applications of Clays in Nanocomposites and Ceramics," *minerals Review*, vol. 14, no. 93, pp. 1–15, 2024.

[16] S. Khandelwal, V. Dhand, J. Bae, T. Kim, and S. Kim, "Influence of Calcination and Cation Exchange (APTES) of Bentonite - Modified Reinforced Basalt / Epoxy Multiscale Composites ' Mechanical and Wear Performance : A Comparative Study," *Materials*, vol. 17, no. 4760, pp. 1–11, 2024.

[17] A. Feriancová, A. Dubec, J. Pagáčová, and M. Pajtášová, "Modification of the Filler based on Kaolin and its Use in the Polymer Composites," *MATEC Web of Conferences*, vol. 357, no. 07004, pp. 1–11, 2022.

[18] K. Boakye, "Influence of Calcined Clay Pozzolan and Aggregate Size on the Mechanical and Durability Properties Pervious Concrete Influence of Calcined Clay Pozzolan and Aggregate Size on the Mechanical and Durability Properties of Pervious Concrete," *Journal of Composites Sciences*, vol. 7, no. 182, pp. 1–16, 2023, doi: 10.3390/jcs7050182.

[19] Y. Yuan *et al.*, "Surface Modification of Calcined Kaolinite for Enhanced Solvent Dispersion and Mechanical Properties in Polybutylene Adipate/ Terephthalate Composites," *Molecule*, vol. 29, pp. 1–13, 2024.

[20] M. Pokhriyal and P. Kumar, "Mechanical and microstructural behaviour of NaOH treated Himalayacalamus falconeri fibers as biodegradable reinforcing material in polymer based composites Materials Today : Proceedings Mechanical and microstructural behaviour of NaOH treated Himalayacala," *Materials Today: Proceedings*, no. April, pp. 1–6, 2022, doi: 10.1016/j.matpr.2022.04.295.

[21] N. Herlina Sari, I. N. G. Wardana, Y. S. Irawan, and E. Siswanto, "Characterization of the Chemical, Physical, and Mechanical Properties of NaOH-treated Natural Cellulosic Fibers from Corn Husks," *Journal of Natural Fibers*, vol. 15, no. 4, pp. 545–558, 2018, doi: 10.1080/15440478.2017.1349707.

[22] K. Sangeetha and M. Bhuvaneshwari, "Investigation of Physical, Chemical and Structural Characterization of Eichhornia crassipes Fiber," in *International Conference on Information Engineering, Management and Security 2016 (ICIEMS 2016)*, 1st ed., 2016, ch. Chapter: I, pp. 92–96.

[23] F.-E.- Karim, M. R. Islam, R. Ahmed, A. B. Siddique, and H. A. Begum, "Extraction and characterization of a newly developed cellulose enriched sustainable natural fiber from the epidermis of Mikania micrantha," *Heliyon*, vol. 9, no. 9, p. e19360, Sep. 2023, doi: 10.1016/j.heliyon.2023.e19360.

[24] A. Muhammad, K. C. Thienel, and S. Scherb, "Calcined Clays from Nigeria—Properties and Performance of Supplementary Cementitious Materials Suitable for Producing Level 1

Concrete," *Materials*, vol. 16, no. 7, 2023, doi: 10.3390/ma16072684.

[25] V. Shah, A. Parashar, G. Mishra, S. Medepalli, S. Krishnan, and S. Bishnoi, "Influence of cement replacement by limestone calcined clay pozzolan on the engineering properties of mortar and concrete," *Advances in Cement Research*, vol. 32, no. 3, pp. 101–111, 2020, doi: 10.1680/jadcr.18.00073.

[26] H. Xue, X. Dong, Y. Fan, X. Ma, and S. Yao, "Study of Structural Transformation and Chemical Reactivity of Kaolinite-Based High Ash Slime during Calcination," *minerals Article*, vol. 13, no. 466, pp. 1–17, 2023.

[27] I. Sánchez, I. S. de Soto, M. Casas, R. Vigil de la Villa, and R. García-Giménez, "Evolution of Metakaolin Thermal and Chemical Activation from Natural Kaolin," *Minerals*, vol. 10, no. 6, p. 534, 2020, doi: 10.3390/min10060534.

[28] K. C. Onyelowe *et al.*, "Characterization of net-zero pozzolanic potential of thermally-derived metakaolin samples for sustainable carbon neutrality construction," *Scientific Reports*, vol. 13, no. 1, pp. 1–11, 2023, doi: 10.1038/s41598-023-46362-y.

[29] E. F. Irassar, V. L. Bonavetti, G. P. Cordoba, H. A. Donza, V. F. Rahhal, and C. C. Castellano, "Performance of Composite Portland Cements with Calcined Illite Clay and Limestone Filler Produced by Industrial Intergrinding," *Minerals*, vol. 13, no. 240, pp. 1–27, 2023.

[30] G. Habert *et al.*, "Review of concrete solutions for concrete's environmental impacts," *Nature Reviews Earth & Environment*, vol. 1, no. 11, pp. 559–573, 2020.

[31] F. Zunino *et al.*, "Hydration and mixture design of calcined clay blended cements : review by the RILEM TC 282-CCL," *Materials and Structures*, vol. 1, pp. 1–24, 2022, doi: 10.1617/s11527-022-02060-1.

[32] R. Derouiche, M. Zribi, and S. Baklouti, "Study of Carbonated Clay-Based Phosphate Geopolymer : Effect of Calcite and Calcination Temperature," *Minerals*, vol. 13, no. 284, pp. 1–21, 2023.

[33] K. M. Anove *et al.*, "Physico-Chemical and Mineralogical Characterizations of Two Togolese Clays for Geopolymer Synthesis," *Journal of Min- erals and Materials Characterization and Engineering,* vol. 10, pp. 400–409, 2022, doi: 10.4236/jmmce.2022.105028.

[34] S. A. Shakrani, A. Ayob, M. Asri, A. B. Rahim, and S. Alias, "Structural Order-Disorder Analysis of Thermally-Activated Water-Washed Kaolin Particles Using Fourier Transform Infrared Spectroscopy," vol. 6, pp. 45–52, 2024, doi: 10.4028/p-10dRdD.

[35] F. Zunino and K. Scrivener, "Reactivity of kaolinitic clays calcined in the 650 ° C – 1050 ° C temperature range : Towards a robust assessment of overcalcination Reactivity of kaolinitic clays calcined in the 650 ◦ C – 1050 ◦ C temperature range : Towards a robust assessment of overc," *Cement and Concrete Composites*, vol. 146, no. December 2023, p. 105380, 2024, doi: 10.1016/j.cemconcomp.2023.105380.

[36] X. Gu and Y. Ling, "Characterization and properties of Chinese red clay for use as ceramic and construction materials," *Science Progress*, vol. 107, no. 1, pp. 1–17, 2024, doi: 10.1177/00368504241232534.

[37] S. Nasiri, R. Madandoust, and M. M. Ranjbar, "Investigating the Calcination Temperature and Grinding Time of Calcined Clay on the Mechanical Properties and Durability," *Infrastructures*, vol. 8, no. 139, pp. 1–20, 2023.

[38] Y. Wang, T. Kim, R. Lin, J. Li, and X. Wang, "Developments in the Built Environment Improved high-temperature resistance of limestone calcined clay cement (LC 3) paste with biochar : Multiscale evaluation and mechanistic analysis," *Developments in the Built Environment*, vol. 18, no. March, p. 100403, 2024, doi: 10.1016/j.dibe.2024.100403.

[39] N. Salahudeen, "Metakaolinization Effect on the Thermal and Physiochemical Propperties of Kankara Kaolin," *KMUTNB Int J Appl Sci Technol*, vol. 11, no. 2, pp. 127–135, 2018, doi: 10.14416/j.ijast.2018.04.003.

[40] D. Kosmidi, C. Panagiotopoulou, P. Angelopoulos, and M. Taxiarchou, "Thermal Activation of Kaolin : Effect of Kaolin Mineralogy on the Activation Process †," *Materials proceedings*, vol. 5, no. 18, pp. 1–8, 2021.

[41] P. Alfonso, L. A. Penedo, S. Martínez, A. Martínez, and J. E. Trujillo, "Thermal behaviour of kaolinitic raw materials from San José (Oruro , Bolivia)," *Journal of Thermal Analysis and Calorimetry*, vol. 147, no. 9, pp. 5413–5421, 2022, doi: 10.1007/s10973-022-11245-3.